

## RESEARCH ARTICLE

# Characterization of microparticles derived from waste plastics and their bio-interaction with human lung A549 cells

Rossella Bengalli<sup>1</sup>  | Alessandra Zerboni<sup>1</sup> | Patrizia Bonfanti<sup>1</sup> | Melissa Saibene<sup>1</sup> | Dora Mehn<sup>2</sup> | Claudia Cella<sup>2</sup> | Jessica Ponti<sup>2</sup> | Rita La Spina<sup>2</sup> | Paride Mantecca<sup>1</sup> 

<sup>1</sup>POLARIS Reaserch Center, Department of Earth and Environmental Sciences, University of Milano – Bicocca, Milan, Italy

<sup>2</sup>Joint Research Centre (JRC), European Commission, Ispra, Italy

## Correspondence

Rossella Bengalli, POLARIS Reaserch Center, Department of Earth and Environmental Sciences, University of Milano – Bicocca, Piazza della Scienza 1, Milan 20126, Italy.  
Email: [rossella.bengalli@unimib.it](mailto:rossella.bengalli@unimib.it)

## Funding information

This work was supported by ECOPAVE Project, *Call Accordi per la Ricerca e l'Innovazione cofin.* POR FESR 2014-2020, Regione Lombardia.

## Abstract

Microplastics (MPs) represent a worldwide emerging relevant concern toward human and environmental health due to their intentional or unintentional release. Human exposure to MPs by inhalation is predicted to be among the most hazardous. MPs include both engineered, or primary MPs, and secondary MPs, materials obtained by fragmentation from any plastic good. The major part of the environmental MPs is constituted by the second ones that are irregular in size, shape and composition. These features make the study of the biological impact of heterogenous MPs of extremely high relevance to better estimate the real toxicological hazards of these materials on human and environmental organisms. The smallest fractions of plastic granules, relying on the micron-sized scale, can be considered as the most abundant component of the environmental MPs, and for this reason, they are typically used to perform toxicity tests using in vitro systems representative of an inhalation exposure scenario. In the present work, MPs obtained from industrial treatment of waste plastics (wMPs < 50 µm) were investigated, and after the physico-chemical characterization, the cytotoxic, inflammatory and genotoxic responses, as well as the modality of wMPs interactions with alveolar lung cells, were determined. Obtained results indicated that, at high concentrations (100 µg/ml) and prolonged exposure time (48 h), wMPs affect biological responses by inducing inflammation and genotoxicity, as a result of the cell–wMP interactions, also including the uptake of the smaller particles.

## KEYWORDS

environmental health, genotoxicity, in vitro toxicity, microplastics, plastic wastes, Raman microscopy

## 1 | INTRODUCTION

Microplastics (MPs) represent a worldwide emerging relevant concern toward human and environmental health due to their intentional or unintentional release (Campanale et al., 2020; Shim &

Thomposon, 2015). Most of the plastic becomes waste after disposal and large plastics can slowly biodegrade or break down into small particles in the environment after weathering and ultraviolet (UV) radiation. Due to their high durability, contamination from MPs will persist in the environment for several years (Worm et al., 2017),

This is an open access article under the terms of the [Creative Commons Attribution-NonCommercial-NoDerivs](https://creativecommons.org/licenses/by-nc-nd/4.0/) License, which permits use and distribution in any medium, provided the original work is properly cited, the use is non-commercial and no modifications or adaptations are made.

© 2022 The Authors. *Journal of Applied Toxicology* published by John Wiley & Sons Ltd.

leading to an increased environmental and human exposure to such materials (Andrady, 2011a; Prata, 2018; Shim & Thomposon, 2015).

MPs are commonly defined as particles of plastics having dimensions below 5 mm (Fendall & Sewell, 2009; Moore, 2008) that could be divided in large microplastic (2–5 mm) and small microplastic particles (0.2–2 mm) (Collignon et al., 2014). Nanoplastics are defined as below 1,000 nm, while other authors set the size limit at 100 nm (Gigault et al., 2018). Depending on their origin, MPs are classified as engineered or primary MPs (such as microbeads in toothpaste or cosmetics) and secondary MPs, materials obtained by fragmentation from any plastic goods. The major part of the environmental MPs is constituted by the second ones, and their spread is almost impossible to control. Due to their nature, secondary MPs are irregular in size, shape and composition, and these characteristics make the study of the biological impact of heterogenous MPs of extremely high relevance to better estimate the real toxicological hazards deriving from human and environmental organisms exposure.

Most of the current research is focused on the environmental effects of MPs, especially in the water compartment. Few data are nowadays available about the effects of these materials on human health. Some studies are focused on ingested microplastics and nanoplastics that could contaminate food and water (Barboza et al., 2018; EFSA Panel on Contaminants in the Food Chain, CONTAM, 2016; Schymanski et al., 2018). Nevertheless, the inhalation of airborne particles remains one of the major routes of exposure to microplastics and nanoparticles, including the polymeric ones. One of the main difficulties in assessing the potential effects of inhalable microplastic on human health in real exposure scenarios is the sampling site, the method of collection and the season of sampling (Prata, 2018; Prata et al., 2020). Inhalation can occur from the release of plastic from materials (abrasion) or during their synthesis.

A large contribution to plastic pollution derives from the production of plastic textile fibres and the consequent release of fibrous MPs in the environment (Dris et al., 2017). Secondary MPs can be also derived from sea-salt aerosol formation: Many of the MPs found in the aquatic compartment have a density lower than seawater; thus, they may be transported as sea-salt aerosols through sea-spray and wind action to urban environments located near to the coast (Wright & Kelly, 2017).

Last but not least, most of the plastic materials end up in landfills since they are usually unrecyclable. Nevertheless, there are efforts in reusing and recycling MPs in order to apply a sustainable approach (European Commission, 2018). In this perspective, waste from plastics otherwise sent to incinerators could be used as an alternative fuel for cement industry (Asamany et al., 2017) or as an additive in the production of conglomerates for the surface treatment of urban and rural roads (Capuano et al., 2020; EAPA, 2017; Grady, 2021). Obviously, since roads' abrasion can occur (Amato et al., 2012; Sommer et al., 2018), the use of waste plastics as road component has posed a great concern about the possible release of these materials in the atmosphere and consequent human exposure. Plastic-waste management procedures could be associated with occupational and

environmental risks, especially when they are subjected to shredding and grinding.

Most of the researches on the microplastics health effects are nowadays focused on synthetic and standard commercial MPs, including PS (polystyrene), PE (polyethylene) and PP (polypropylene) plastic, but waste plastics, used in thermovalorization plants or for recycling processes, are actually composed of different variety of plastics. Furthermore, it is important to mention that, besides compounds related to plastic composition, MPs may also adsorb and release environmental contaminants due to their large surface area and hydrophobicity (Teuten et al., 2007; Wang et al., 2018).

Data on the effects of inhaled MPs on humans are scanty. Wright and Kelly (2017) reviewed the evidence of the possible effects of MPs in the respiratory system. Recently, studies support the idea of airborne contamination, by the identification of MPs in the atmospheric fallout of a city (Dris et al., 2015, 2016).

Nevertheless, more efforts should be done in order to better characterize MPs and their physical-chemical properties, as well as to monitor their real environmental concentrations and to understand the possible mechanisms of toxicity related to MPs exposure.

In this work, a widely used *in vitro* model of the human lung epithelium, A549 cells, was used to evaluate the possible toxic effects on inhalable plastic-waste derived MPs (wMPs). As biological endpoints, cytotoxicity, inflammatory response, bio-interaction among cells and wMPs and genotoxicity were investigated after the exposure to micro-sized (<50 µm) wMPs, which were previously characterized by microscopic and spectroscopic techniques. The obtained results highlighted the importance to improve the studies on the characteristics and the biological modes of action of the highly heterogeneous environmental MPs.

## 2 | MATERIAL AND METHODS

### 2.1 | Microplastics collection and characterization

The microparticles from plastic waste (wMP) were recovered in the laboratory from industrially recycled plastic granules, as previously reported (Bonfanti et al., 2021). As part of the ECOPAVE project, a pilot value chain was set up by industrial partners to collect and reuse non-recyclable plastic waste. In short, plastic waste of various origins was collected separately in ecological platforms, manually separated from any metal parts and transferred to a plastic recycling plant, where they were further processed by washing treatments to remove impurities and controlled flotation to obtain a fraction of polyolefin-enriched plastics and finally properly ground to obtain a granulated blend with dimensions less than 3 mm.

The obtained plastic granulates were transferred in laboratory and mechanically sieved and grinded using stainless steel sieves with decreasing mesh size (1 mm – 500 µm – 250 µm – 150 µm – 100 µm – 50 µm). The finest fraction achieved, corresponding to nominal MP particle dimensions of <50 µm, was used for *in vitro* toxicity studies after being characterized by Fluorescence and Scanning Electron

Microscopy (FM and SEM, respectively) in term of morphology and by Raman spectroscopy in order to analyse the wMPs chemical composition. If not otherwise specified, a suspension 1 mg/ml of wMPs was prepared in sterile milliQ and used for all the experiments.

### 2.1.1 | Size distribution of wMPs

The size and particle size distribution of wMP fraction were determined by the laser diffraction method (Malvern Mastersizer 3000) and through optical microscopy analysis. For the Mastersizer analysis, samples were dispersed in ethanol and in 0.1% w/v Triton X-100 and kept under continuous stirring (850 rpm) during the analysis. Each measurement was performed in five replicates to ensure consistency of the results. The model for data analysis assumes that the particles are not-spherical, while refractive and absorption indexes were set to 1.5 and 0.010, respectively. Laser obscuration was kept in the range between 10% and 20%.

The size distribution of wMPs conducted by optical microscopy analysis was represented as distribution of min Feret Diameter (Walton, 1948). MPs suspended in ethanol were dropped on a silicon wafer and analysed with a Zeiss Axioplan microscope equipped with an Axiocam MRC5 digital camera. Several images were acquired in Bright Field. The images were then analysed using NanoDefine ParticleSizer software (ImageJ Plugins), in order to automatically determine the size distribution of the wMPs.

### 2.1.2 | Fluorescence microscopy and Nile Red staining

For the FM analysis, small amounts of wMPs (50  $\mu$ l) at 1 mg/ml were mounted onto glass slides and observed with a Zeiss Axioplan microscope equipped with an Axiocam MRC5 digital camera. Furthermore, in order to better visualize wMPs, particles were also stained with the dye Nile Red (Merck KGaA, Darmstadt, Germany). Nile Red (NR) stock solution was prepared at 1 g L<sup>-1</sup> in acetone (Merck KGaD) and vacuum filtered using pore size 0.1  $\mu$ m Whatman<sup>®</sup> Anodisc inorganic filter membrane with a diameter of 25 mm. The staining was carried out by adding 100  $\mu$ l of NR stock to a solution of 5 ml methanol (Merck KGaD) and 5 ml of milliQ water to give a final of 10  $\mu$ g ml<sup>-1</sup> NR in the suspension of wMPs. An exposure time of 30 min was used (Maes et al., 2017). The suspension was then vacuum filtered (Whatman<sup>®</sup> 25 mm Anodisc inorganic filter membrane, pore size 0.1  $\mu$ m), rinsed with 30 ml methanol and left to dry. The stained wMPs were then analysed by fluorescent microscope (Zeiss, Axio Imager) under green (filter 488009-9901-000, excitation/emission 460/525 nm) and red (filter 89060-9901-000, excitation/emission 565/630 nm) light.

### 2.1.3 | SEM analyses

In order to analyse wMPs with Scanning Electron Microscopy (SEM), a small aliquot of sample (50  $\mu$ l) was deposited on SEM stub with

conductive carbon tape and let dry. Samples were then sputter coated with 10 nm of chromium and observed with High-Resolution Field-Emission SEM Zeiss Gemini 500 operating at 3 kV acceleration voltage in order to preserve plastic material and to get a good resolution of particles surface.

## 2.2 | Raman spectroscopy of wMPs

wMPs were deposited on polished, clean silicon support without any further treatment. Raman spectroscopic analysis of the particles was performed using an alpha300 confocal Raman microscope (WITec, Ulm, Germany) equipped with a 532 nm laser. Raman spectra were collected using a 10X objective typically at 10  $\times$  1 s integration time. Identification of the spectra was done after baseline subtraction using the ACDLabs UVVis manager and in some cases (polyethylene copolymer) the open spectral database OpenSpecy ([www.openspecy.org](http://www.openspecy.org)) (Cowger et al., 2021). Spectra with no specific Raman features (only wide fluorescent signal) were considered to be non-identified.

## 2.3 | Endotoxin quantification

Limulus amoebocyte lysate (LAL) test was performed on the wMPs sample using a LAL Chromogenic Endotoxin Quantitation Kit (Thermo Scientific<sup>™</sup> Pierce<sup>™</sup>), following the manufacturer's instructions and working with endotoxin-free materials and in sterile condition. Samples are mixed with the LAL reagent in a 96-well plate, and the absorbance of each sample was measured using a Multiplate Reader Ascent (Thermo Scientific, USA) at the wavelength of 405–410 nm. The amount of endotoxin present in the sample can be calculated using a standard curve and express as EU/ml.

## 2.4 | Cell culture maintenance and treatments

Human alveolar epithelial cells (A549 cell line, ATCC<sup>®</sup> CCL-185, American Type Culture Collection, Manassas, VA, US) were cultivated in OptiMEM medium (Gibco, Life Technologies, Monza, Italy) supplemented with 10% foetal bovine serum (FBS; Gibco) and antibiotics (penicillin/streptomycin, 100 U/ml) (Euroclone, Pero, Italy) and maintained in incubator at 37°C and 5% CO<sub>2</sub>. For the evaluation of wMPs in vitro effects, cells were treated with different concentrations of wMPs (0.1, 1, 10 and 100  $\mu$ g/ml) directly adding particles suspension into the medium for different times of exposure (24 or 48 h).

## 2.5 | Cell viability

The cytotoxicity of wMPs on A549 cells was evaluated by the 3-(4,5-dimethylthiazol-2-yl)-2,5-diphenyltetrazolium bromide (MTT) test. Cells were seeded on a six-well multiwell at the density of 1.6  $\times$  10<sup>5</sup> cell/well and after 24 h were treated with different

concentrations of wMPs (0.1, 1, 10, 100 µg/ml), that were added in the culture medium. In untreated cells (control), the volume of particle suspension used for the highest concentration was substituted with same amount of milliQ water added to the culture medium.

MTT (Sigma Aldrich, Milano, Italy) assay was performed according to previous works (Bengalli et al., 2019; Mosmann, 1983). Briefly, at the end of exposure (24 and 48 h), cells were rinsed with phosphate buffered saline (PBS), and MTT solution was added to the medium (final concentration 0.3 mg/ml) for 3 h. After the production of formazan crystals, these were solubilized in Dimethyl sulfoxide (DMSO, Sigma Aldrich), and the absorbance was measured at 570 nm by a multi-plate reader (Infinite 200 Pro, TECAN, Männedorf, Switzerland). The percentage of cell viability was calculated according to the formula: (Absorbance treated sample/Absorbance control sample)\*100.

## 2.6 | Interleukin-8 and Interleukin-6 release

Cells were seeded on a six-well multiwell at the density of  $1.6 \times 10^5$  cell/well and after 24 h were treated with different concentrations of wMPs (0.1, 1, 10, 100 µg/ml). The release of IL-8 and IL-6 from A549 cells was evaluated in the supernatants that were collected after 24 and 48 h of exposure, centrifuged at 1,200 rpm for 6 min and then stored at  $-80^\circ\text{C}$  until analysis. The quantification of cytokines was performed through IL-8 and IL-6 ELISA matched antibody pair kit (Invitrogen, Life Technologies, Monza, Italy) according to the manufacturer's instruction. The absorbance of each sample was measured by a multiplate reader (Infinite 200 Pro, TECAN, Männedorf, Switzerland) at the wavelength of 450 nm, and the amount of proteins was calculated based on standard curves, and data were shown as pg/ml.

## 2.7 | Intracellular ROS detection by flow cytometry

The Intracellular production of reactive oxygen species (ROS) was detected using the probe 2',7'-dichlorodihydrofluorescein diacetate ( $\text{H}_2\text{DCFDA}$ , final concentration 5 µM, Life Technologies, Monza, Italy). A549 cells ( $1.6 \times 10^5$  cells/well) were seeded in six-well plates for 24 h and then loaded with 5 µM  $\text{H}_2\text{DCFDA}$  in PBS 1X for 20 min at  $37^\circ\text{C}$ . Thereafter, cells were washed twice with PBS, incubated with wMPs (0.1–100 µg/ml) for 24 h. Then, after washing with PBS twice, cells were harvested and analysed by cytofluorimeter (CytoFLEX, Beckman Coulter, Milano, Italy) with excitation and emission settings of 488 and 525 nm. The possible interference of wMPs was assessed analysing the signal from samples (cells treated with wMPs at the different concentrations and washed as above) not stained with  $\text{H}_2\text{DCFDA}$ . These values were then subtracted from the values to  $\text{H}_2\text{DCFDA}$  stained samples.

## 2.8 | Cytokinesis-block micronucleus assay

The first day, A549 cells were seeded on a six-well plate at the density of  $1.2 \times 10^5$  cells/well; on the second day, cells were treated with wMPs (100 µg/ml) for 48 h; Mitomycin C (MMC) (Sigma-Aldrich) was used as a positive control at a final concentration of 0.7 µM. After 48 h of exposure, the medium was removed, and cells were gently washed twice with pre-warmed PBS, and then, Cytochalasin B (Sigma-Aldrich) was added to each well at a final concentration of 1.5 µg/ml, and cells were incubated for an additional 26 h. At the end of incubation in the presence of Cytochalasin B, the medium was removed and each well gently washed twice with pre-warmed PBS. Cells were harvested with Trypsin-EDTA solution (Life Technologies) and centrifuged for 5 min at room temperature (RT), at 1,000 rpm (Eppendorf 5810R centrifuge, rotor A-4-62). After the removal of the supernatant, a pre-fixing solution of ethanol: glacial acetic acid (6:1) was added to the cells and incubated for 2 min at RT. Then, after centrifugation, ice-cold ethanol was added to the cells and incubated for 1 h at  $-20^\circ\text{C}$ . This procedure was repeated three times. The fixed cells were then re-suspended gently with a glass Pasteur pipette and dropped on cold microscope slides. The slides were let dry for at least 6 h and then stained with a solution of 2% Giemsa. Samples were then processed and analysed according to the criteria of Fenech and OECD guidelines (Fenech, 2007; OECD, 2016). Three biological replicates for each sample were prepared for cytokinesis-block micronucleus (CBMN) analysis with two technical replicates each. For each experimental condition, the cytokinesis block proliferation index (CBPI) was calculated using the following formula:  $((N^\circ \text{ mononucleated cells}) + (2 \times N^\circ \text{ binucleated cells}) + (3 \times N^\circ \text{ multinucleated cells})) / (\text{total number of cells})$ . Furthermore, for each experimental condition the number of micronuclei and nuclear buds in 1,000 binucleated cells was evaluated.

## 2.9 | Morphological changes

For morphological analysis, cells were seeded on a cover slide at a concentration of  $1.5 \times 10^5$  cells/well, cultured for 24 h and then exposed to wMPs (100 µg/ml, with and w/o Nile Red staining) for further 24 or 48 h. At the end of the treatment, cells were washed twice with PBS and then fixed in 4% paraformaldehyde for 20 min, washed and permeabilized with 0.1% Triton-100X and then incubated with rhodamin-phalloidine for 30 min (1:40 dilution, Cytoskeleton Inc., Denver, CO, USA) for the analyses of cytoskeleton organization. After PBS washing, nuclei were counterstained with DAPI (dilution 1:350) and after PBS washing slides were mounted with ProLong™ Gold Antifade Mountant (Molecular Probe, Life Technologies, Monza, Italy), dried o/n and then observed at the microscope (AxioObserver Z1 Cell Imaging station, Zeiss, Germany). Images were acquired by an MRc5 digital camera and elaborated with the dedicated software (Zeiss ZEN 2.3 Blue edition).

## 2.10 | $\mu$ Raman analysis of cells

A549 cells were seeded on a  $3 \times 3$  mm<sup>2</sup> silicon wafer  $1.2 \times 10^5$  cells/wafer in a 12-well plate. After 24 h, cells were treated with wMPs (100  $\mu$ g/ml). After 48 h of exposure, the medium was removed, and cells were gently washed with pre-warmed PBS, and then, cells were fixed with Karnovsky solution (2%). Raman spectroscopic analysis of cells exposed to wMPs was performed in the fixative solution, using a WITec alpha300 confocal Raman microscope equipped with a 532 nm laser. Raman spectra were collected using a 60X water immersion objective at 1  $\mu$ m lateral resolution, 5  $\mu$ m depth in z-stacking and applying 2 s integration time for each pixel. The intensity of the C-H stretching vibration region was mapped for each of the hyperspectral images to roughly identify the position of nucleus and cytoplasm. Then, average nucleus, cytoplasm and background spectra were generated by averaging the spectra of more pixels. These average spectra were used for base component analysis after cosmic ray removal and baseline subtraction at each pixel of the spectral map. Intensity maps of the components were coloured with blue for nuclei, green for cytoplasm and red for particle(s).

## 2.11 | Transmission electron microscopy analysis of microplastics uptake

A549 cells were exposed to wMPs (100  $\mu$ g/ml), prepared by dilution of 1 mg/ml stock suspension incubated overnight in antibiotics solution (penicillin/streptomycin, 100 U/ml, Euroclone, Pero, Italy), for 24 h and for 48 h. After exposure, cells were washed twice in PBS and fixed in Karnovsky 2% fixative overnight at 4°C. Cells were then washed three times with 0.05 M cacodilate pH 7.3 and post-fixed in osmium tetroxide solution in 0.1 M cacodilate pH 7.3 for 1 h. After three washes in cacodilate 0.05 M of 10 min each, cells were dehydrated in a graded series of ethanol solutions in MilliQ water (30%–50%–75%–95% for 15 min each and 100% for 30 min), incubated in absolute propylene oxide for 20 min (two changes of 10 min each) and embedded in a solution of 1:1 epoxy resin and propylene oxide for 90 min. This mixture was renewed with pure epoxy resin overnight at room temperature and later polymerized at 60°C for 48 h. Ultrathin sections (50–70 nm) were obtained using Leica UCT ultramicrotome (Leica, Italy) and stained for 2 min with UranylLess EM stain (Electron Microscopy Sciences, Hatfield, Pa, USA) and lead citrate solution by Reynolds for other 2 min, washed and dried. Reagents used to prepare solutions, if not specified, were supplied by Sigma Aldrich, Italy. Sections were then collected on Formvar Carbon coated 200 mesh copper grids (Agar Scientific, USA) and imaged by JEOL

JEM-2100 HR-transmission electron microscope at 120 kV (JEOL, Italy).

## 2.12 | Statistical analysis

The data represent the mean  $\pm$  standard error of the mean (SE) of at least three independent experiments. Statistical analyses were performed using GraphPad 6.0v software, using unpaired *t* test or one-way ANOVA and Bonferroni's post hoc analysis, if not elsewhere specified in the figure captions. Values of  $p < 0.05$  were considered statistically significant.

## 3 | RESULTS

### 3.1 | Waste microplastics characterization

Results from Mastersizer analysis for volume size distribution, as reported in Table 1, were obtained for MPs below 50  $\mu$ m (wMPs<50), where  $D_{50}$  represents the median particle size, which means that 50% of the particles shows a size (calculated from the volume distribution) below the reported value. In addition,  $D_{90}$  and  $D_{10}$  mean that 90 and 10% of the particles' size were less than the corresponding values, respectively. Data showed that the 50% of the particles have a mean diameter below 60  $\mu$ m and that less than 10% of particles have a size below 30  $\mu$ m.

Data for size distribution from optical microscope analysis show that the 50% of particles have a diameter below 25  $\mu$ m (Figure S1). Although some particles resulted larger than 50  $\mu$ m, it is noticeable that the most represented wMPs fall in the size range of 5–15  $\mu$ m, a fraction relevant for inhalable particles.

FM images suggest that the wMPs have an irregular shape and they are inherently fluorescent (especially in green and red channels). In order to better analyse wMPs morphology and size distribution, staining with Nile Red, which preferentially absorbs on the hydrophobic surface of plastics, was performed. Nile Red staining improves the fluorescence of the particles (Figure S2), but in the samples, there are some MP particles that are not stained by the dye (the black spot, which are not fluorescent, Figure S2f). The size distribution analysis from MPs stained with Nile Red shows that the size range of the particles is between 20 and 90  $\mu$ m, with an average size of 41.2  $\mu$ m (Figure S3).

Particles were further characterized in terms of shape and dimension by Scanning Electron Microscope (SEM) analysis. SEM images (Figure 1) confirmed that the particles have irregular shape, including

	Dx (10) ( $\mu$ m)	Dx (50) ( $\mu$ m)	Dx (90) ( $\mu$ m)
wMPs < 50 (ethanol)	31.047 $\pm$ 0.029	60.682 $\pm$ 0.236	141.659 $\pm$ 4.660
wMPs < 50 (Triton X-100)	29.618 $\pm$ 0.161	59.595 $\pm$ 0.640	127.334 $\pm$ 8.933

**TABLE 1**  $D_{10}$ ,  $D_{50}$  and  $D_{90}$  values for the volume size distribution of the fractions wMP < 50  $\mu$ m

Note: Data referred to average  $\pm$  SD of five replicates.

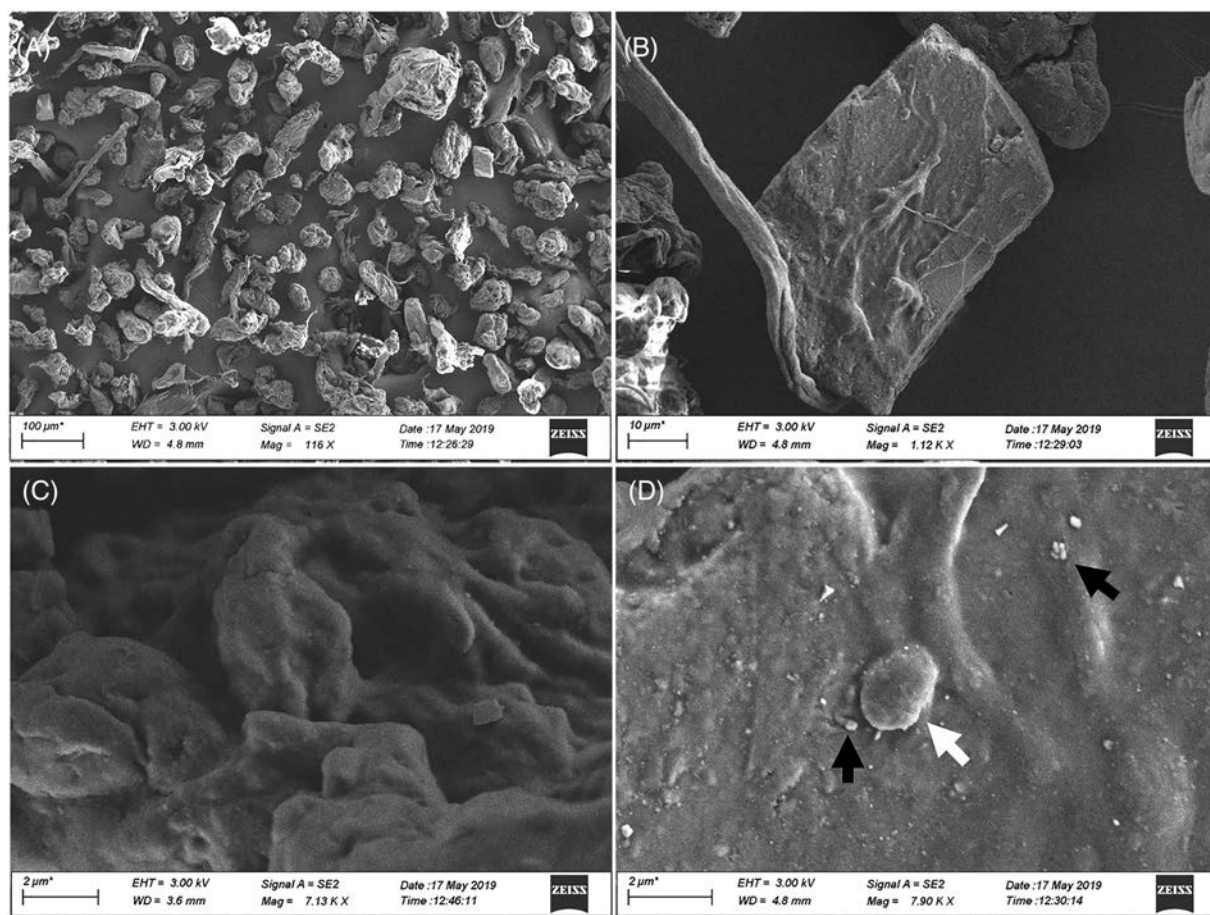


**FIGURE 1** SEM images of wMPs. wMPs morphology was analysed by SEM at low (A, B) and high magnification (C, D). Small dimension wMPs are visible on the surface of the bigger ones, including particles with a diameter of  $\leq 2 \mu\text{m}$  (white arrow) and in the nanosized range (black arrows). Scale bars: (A)  $100 \mu\text{m}$ ; (B)  $10 \mu\text{m}$ ; (C and D)  $2 \mu\text{m}$

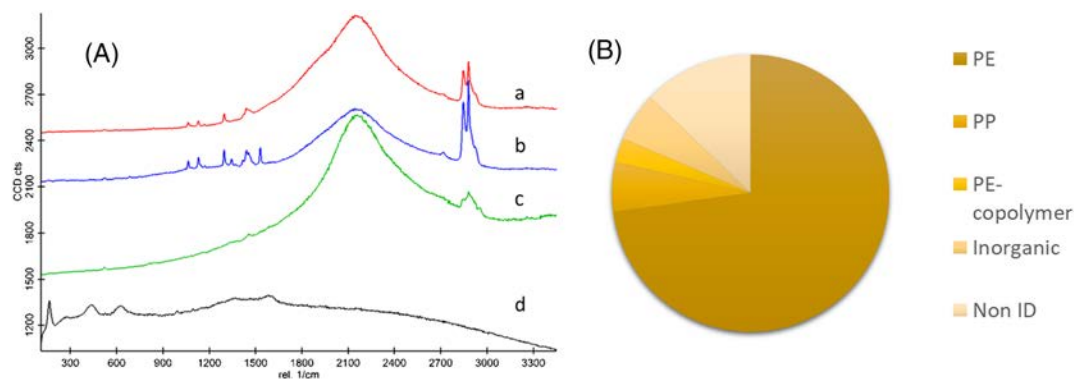


**FIGURE 2** Results of Raman spectroscopic analysis of wMP particles: (A) representative Raman spectra of wMPs identified as (a) PE (red line), (b) PE containing phthalocyanine blue (blue line), (c) PP (green line), (d) particles containing  $\text{TiO}_2$  (black line). (B) Chemical composition of the analysed particles

fibre-like structures, with marked surface roughness and structural defects at submicron scale. In addition, smaller and even nanometre sized particles are recognizable on the surface of the larger wMPs (Figure 1D).

The characterization of the wMPs was performed also by Raman spectroscopy, which allows the identification of the polymeric composition and the compounds present in the wMPs particles. The spectroscopy results showed that most of the particles are fluorescent at

the applied excitation wavelength and this property changes in a very wide range (Figure S4). The analysis of 70 particles showed that about 72% of the particles is most probably PE, 5% is PE copolymer, 3% is PP, 6% is inorganic material, like iron-oxide and TiO<sub>2</sub>, and 12% is unidentified (in most cases because of the strong fluorescent signal). Furthermore, some wMPs contain additives, like titania or phthalocyanine blue, in accordance with previous observations by Simon and colleagues (Simon & Röhrs, 2018) (Figures 2 and S5).

Finally, wMPs were also characterized for the content of endotoxin (lipopolysaccharide) through LAL test. Data showed that the amount of endotoxin in the wMPs samples was of 0.044 ± 0.003 EU/mg.

## 3.2 | In vitro effects of waste microplastics

### 3.2.1 | Cytotoxic and pro-inflammatory effects

A549 cells were exposed to increasing concentrations of wMPs (<50 µm) suspensions and cell viability was assessed after 24 and 48 h by MTT test. After 24 h, there is no significant reduction of cell viability, whereas at 48 h, there is a small reduction of cell viability, of the 12% and 25% respect to the control, at the concentrations of treatment 10 and 100 µg/ml, respectively (Figure 3). Statistically significant reduction of cell viability was observed only at the highest concentration tested. After 24 h of exposure to wMPs, the intracellular ROS level was investigated to see if the cytotoxic effects observed at prolonged time (48 h) could be due to the increased production of oxygen species. At the tested conditions, no increase of intracellular ROS expression was observed (Figure S6).

The inflammatory response induced after exposure of A549 cells to wMPs was assessed by the investigation of IL-8 and IL-6 release after 24 and 48 h of exposure. IL-8 and IL-6 are cytokines involved in inducing a pro-inflammatory status in response to inhaled particles, and IL-8 is also involved in irritation. Data showed that high

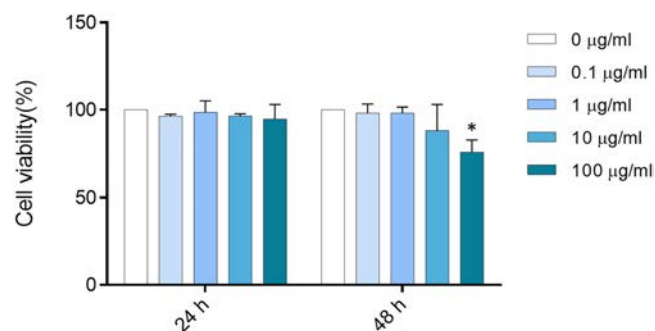


**FIGURE 3** Cell viability. A549 cells were exposed to increasing doses (0, 0.1, 1, 10, and 100 µg/ml) of wMPs for 24 and 48 h. After the exposure, cell viability was assessed by MTT test. Control cells (unexposed) are considered 100% viable. Data represent the mean ± SE of three independent experiments ( $n = 3$ ). \*Statistically different respect to the control,  $p < 0.05$ ; one-way ANOVA + Bonferroni's post hoc test

concentrations (100 µg/ml) of wMPs induced a significant increase in IL-8 release after 48 h of exposure (Figure 4A). A significant increase in the release of IL-6 at 48 h of exposure was also observed, although the protein concentration was very low (Figure 4B).

### 3.2.2 | Genotoxic effects

In order to assess the genotoxic impact of wMPs on A549 cells, the CBMN assay was performed. According to this test, after division, cells appear binucleated (Figure 5A,C,D) due to the blocking of cytokinesis with cytochalasin-B (Fenech, 2007). Micronuclei (MN) (Figure 5C) derive from chromosome fragments or chromosomes lagging behind at anaphase and are markers of chromosome breakage or whole chromosome loss. We observed a significant increase of micronucleus number after the exposure to wMPs respect to the control cells in 1,000 binucleated cells for each sample (Figure 5E). Furthermore, we analysed the presence of Nuclear Buds (Bud) (Figure 5D), which derive from the nucleus associated to micronuclei, or as extroflexions of nucleoplasmic material (OECD, 2016). Nuclear Buds are biomarkers of gene amplification and DNA repair complexes (Thomas et al., 2003). Figure 5F shows that the number of Bud in 1,000 binucleated cells increases, even if not significantly, after the exposure to wMPs. Data obtained from the CBMN test were also analysed calculating the 'Cytokinesis Block Proliferation Index' (CBPI)

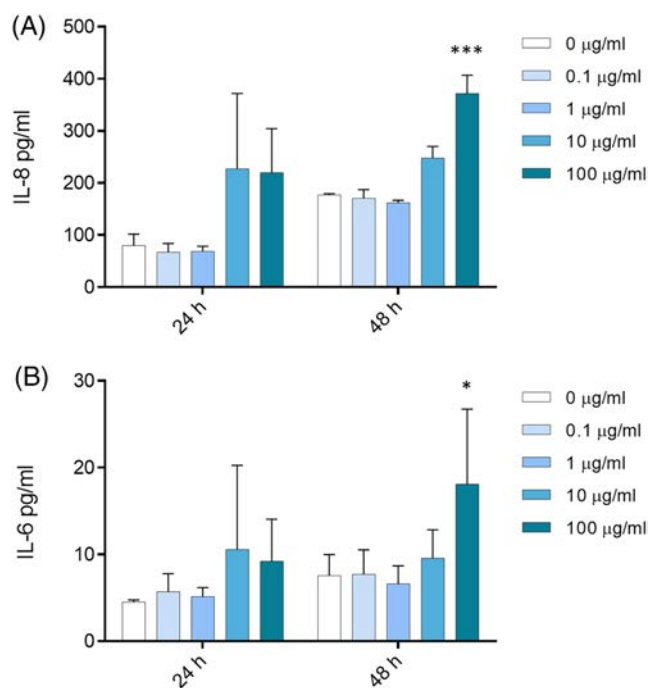


**FIGURE 4** Inflammatory response. Release of IL-8 (A) and IL-6 cytokines (B) from A549 cells after 24 and 48 h of the exposure to increasing doses (0, 0.1, 1, 10, and 100 µg/ml) of wMPs. Data represent the mean ± SE of three independent experiments ( $n = 3$ ). \*Statistically different respect to the control; \*\*\* $p < 0.001$ ; \* $p < 0.05$ , one-way ANOVA + Bonferroni's post hoc test

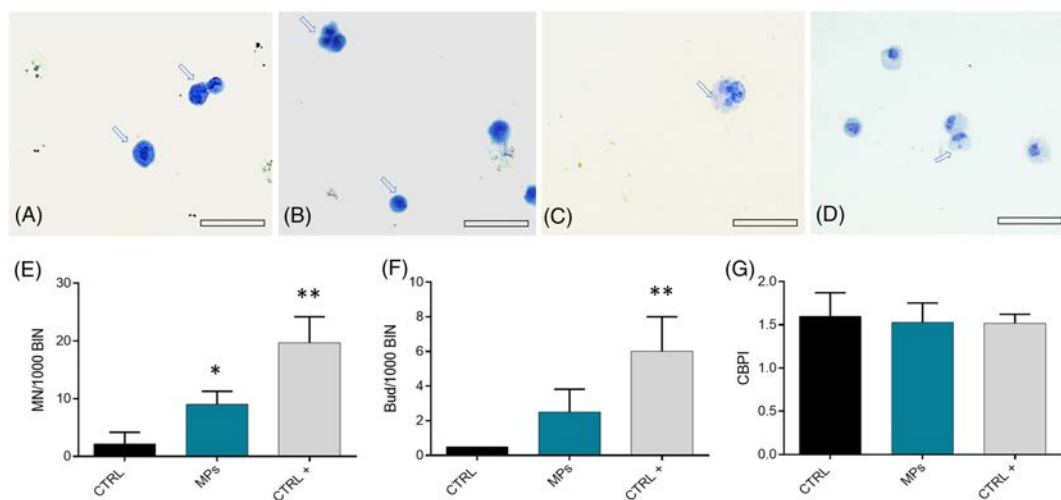


**FIGURE 5** Cytokinesis-block micronucleus (CBMN) assay in the A549 cells: genotoxicity evaluation after wMPs exposure. (A) Binucleated cells; (B) polynucleated and mononucleated cells; (C) binucleated cells with micronuclei (MN); and (D) binucleated (BIN) cells with nuclear buds (BUDs); (E) number of MN in 1,000 binucleated cells (MN/1000 BIN) in A549 cells after 48 h of exposure to 100  $\mu\text{g}/\text{ml}$  of wMPs; (F) number of Bud in 1,000 binucleated cells (Bud/1,000 BIN) in A549 cells evaluated after 48 h of exposure to 100  $\mu\text{g}/\text{ml}$  of wMPs; (G) Cytokinesis Block Proliferation Index (CBPI) calculated in A549 cells exposed to 100  $\mu\text{g}/\text{ml}$  of wMPs for 48 h. Untreated cells were used as control (CTRL); mytomicin C (0.7  $\mu\text{M}$ ) was used as a positive control (CTRL+). Mean  $\pm$  SE of three replicas ( $n = 3$ ). \*Statistically different respect to the CTRL; \* $p < 0.05$ ; \*\* $p < 0.005$ , according to unpaired Student  $t$  test. Scale bar = 100  $\mu\text{m}$

to evaluate the cellular proliferation progression, and therefore the cytostatic effects, after exposure to wMPs 100  $\mu\text{g}/\text{ml}$  for 48 h. The CBPI obtained from the cells treated with the wMPs is not modified respect to control (Figure 5G).

### 3.2.3 | Cell-wMPs bio-interactions

Actin staining on cells was performed in order to analyse the effect of wMPs exposure on cellular morphology (Figure S7). A549 cells were treated for 24 and 48 h with the highest concentration of wMPs (100  $\mu\text{g}/\text{ml}$ ), then stained with rhodamine-phalloidin for actin detection and observed at fluorescence microscopy. Nuclei were stained with DAPI. wMPs stained with Nile Red protocol were also used in parallel to make the wMPs identification easier.

Treated cells, both at 24 and 48 h, showed an altered morphology compared to the untreated cells, with disassembled cytoskeleton and ruffled actin filaments. We observed micronuclei (MN) and nuclear buds (NBDs) formation indicate cell stress and DNA damage after wMPs exposure, as well as some cells that undergo to mitotic catastrophe (Figure S8), sustaining the results of Section 3.2.2. By fluorescent microscopy, it was possible to map micrometre-sized wMPs (with or without Nile Red staining) in contact with cells (Figure S7e, f). It is noteworthy that the amount of wMPs adhering or being internalized in cells was very low in respect to the high concentration used.

Data of  $\mu\text{Raman}$  imaging and analysis showed that particles with strong fluorescent signal were found in cells, inside the cytoplasm (Figure 6) and, in some cases, near to the nucleus (Figures S9 and S10), as confirmed by the z-stack analysis. The fluorescent signal of these particles detected by the sensitive CCD camera of a Raman

spectrometer unfortunately hides the specific Raman features of the polymers. In the absence of other intentionally added fluorescent material, we can speculate that the fluorescent objects are wMP particles, even if we cannot consider this as a direct evidence for the presence of wMPs inside the cells.

TEM results (Figure 7) confirm the confocal and  $\mu\text{Raman}$  microscopic mapping finding plastics inside cells. Plastics fragments of around 1–2  $\mu\text{m}$  or less are observed inside cells more in the cytoplasm environment, sometimes near the nucleus (Figure 7B,D,G) and in some cases following the internal membrane structure (Figure 7C,D) in few cases inside endosomes (Figure 7G). This observation could suggest a direct mechanism of interaction and uptake such as a microplastics attachment to the cell membrane and a sort of endo-phagocytosis, not receptor mediated, or direct injection of sharp materials into cells.

## 4 | DISCUSSION

Although MPs are contaminants of emerging concern, there is little information available about the toxicity of environmental airborne MPs and their effects on the respiratory system. Particles deposition on deep lung seems attributable only to inhaled particles with size below 5  $\mu\text{m}$  (Gasperi et al., 2018); however, micrometric MPs can be found as substances in the organic fraction of atmospheric particulate matter (PM) (Prata, 2018).

In this work, for the first time, the toxic effect of environmentally relevant MPs mixtures deriving from waste (wMPs) and below 50  $\mu\text{m}$  in size was investigated in human pulmonary cells.

Fractions were separated based on defined sieve mesh size and, due to the limitation in the separation of the smallest fraction of

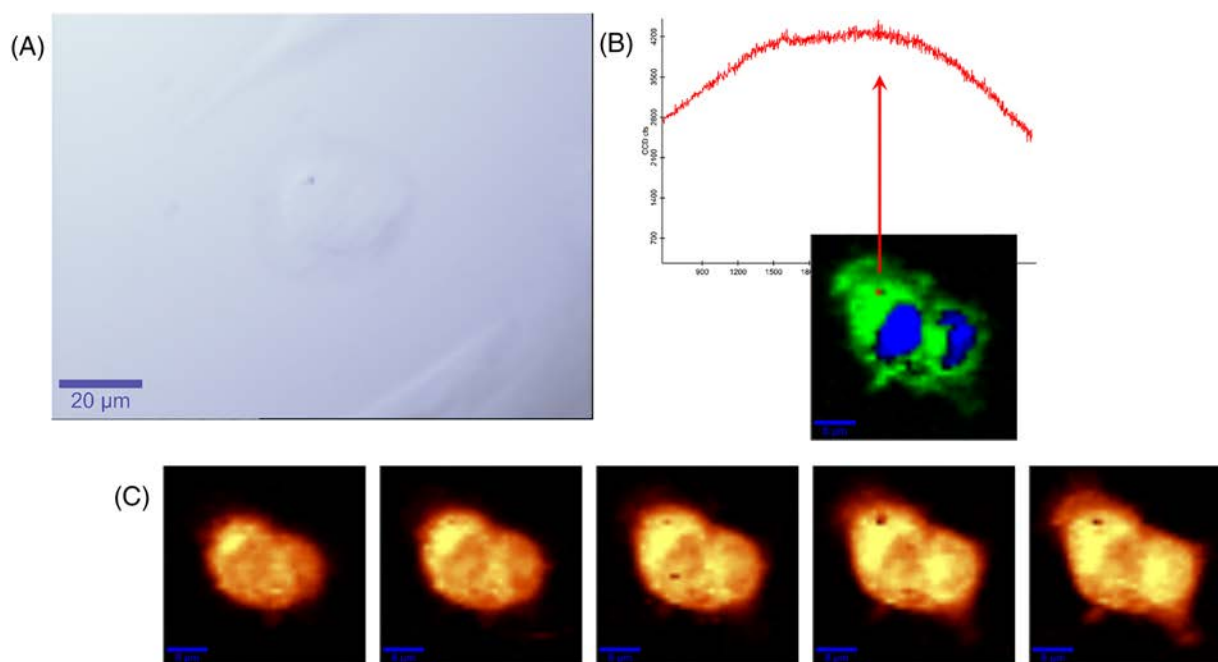


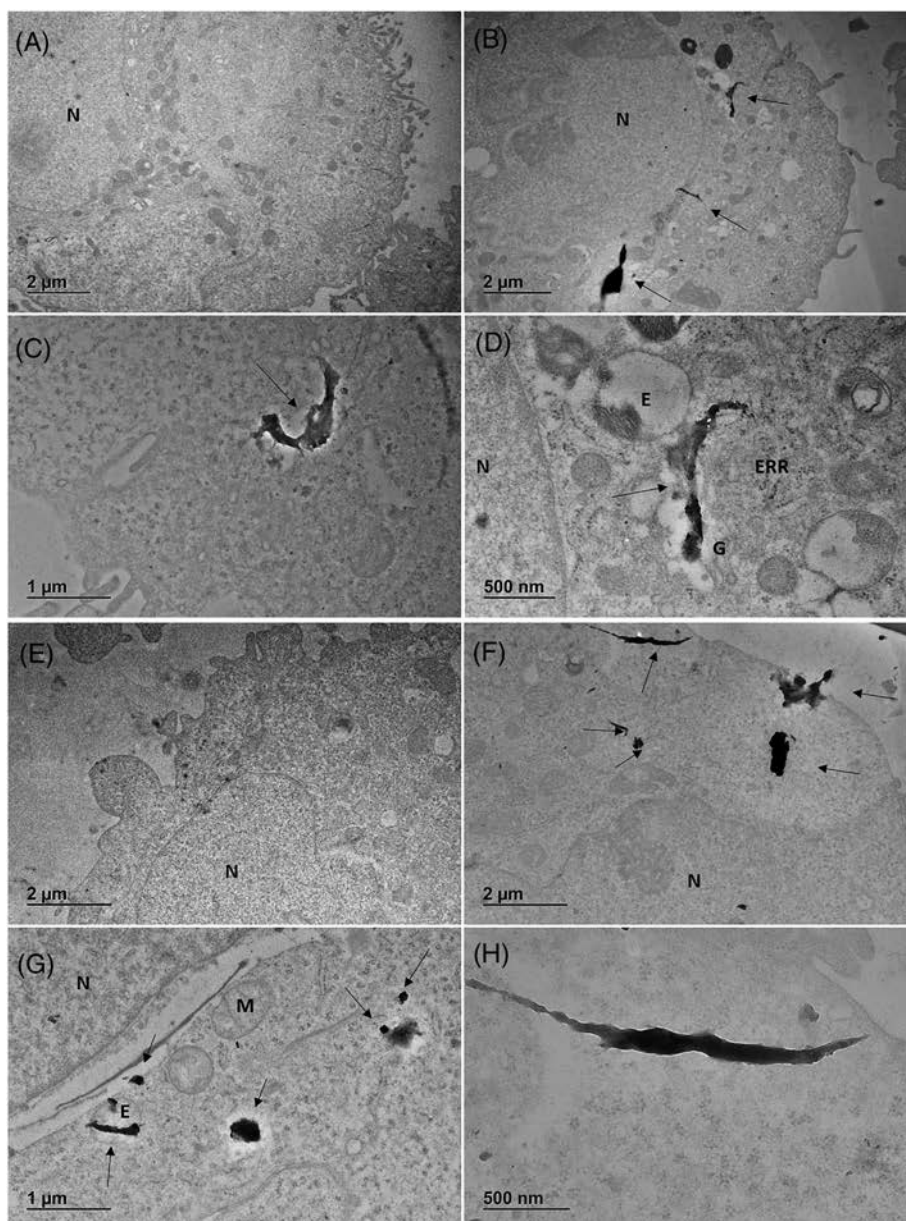
**FIGURE 6**  $\mu$ Raman microscopic mapping of cells. (A) Optical image (60X water immersion objective, scale bar 20  $\mu$ m); (B) Raman spectra of wMPs (up, red line) and false colour chemical image of cells (down, green cytoplasm and blue nuclei); (C) intensity map of the C-H stretching vibration spectral region, Z stack of a 5  $\mu$ m thick slice (scale bar 10  $\mu$ m)

wMPs, we decided to use the fraction of wMPs < 50  $\mu$ m as representative of the environmental MPs that can interact at higher probability with the respiratory system. On the other hand, testing wMPs of size larger than 50  $\mu$ m on cultured cells is not feasible, while the use of heterogeneous sized particles, smaller than 50  $\mu$ m, with a significant fraction below 20  $\mu$ m, might be relevant to more closely resemble a realistic exposure to environmental MPs; indeed, it has been reported that most of the MPs fragments in the atmospheric PM are below 300  $\mu$ m in size, with a high percentage of MPs having a size below 25  $\mu$ m and among 25 and 50  $\mu$ m (Allen et al., 2019; Cai et al., 2017; Dris et al., 2017).

In this work, size distribution analysis of the selected fraction indicated that wMPs were effectively below 40–60  $\mu$ m, with an average size of 25  $\mu$ m, even if a portion of these particles was below 10 and 5  $\mu$ m. Furthermore, SEM images showed irregular particles in the nanosized range on the surface of the wMPs that could detach from MPs and interact with cells. The irregular size and shape of the wMPs observed by SEM analyses was confirmed also by Nile-Red staining. The lipophilic dye Nile red has been introduced in the analysis of MPs by Andrady (Andrady, 2011b), and it has been adapted and modified by other authors (Erni-Cassola et al., 2017; Maes et al., 2017; Matthias & Hengstmann, 2017; Shim et al., 2016) providing an alternative identification method for MPs. However, Stanton et al. (2019) showed that Nile Red does not reliably stain all plastic particles, due the presence of plastic dyes that may affect their affinity with the fluorescent probe, suggesting that additional analyses and detection techniques are needed to better identify and characterize wMPs, as well as any additional impurities present in the sample.

Information regarding the chemical identity of the particles and the presence of additives and contaminants were obtained using Raman Spectroscopy, which evidenced that the major contributor to wMPs is polyethylene (PE). PE is the most broadly used type of plastic and commonly employed as a manufacturing material for bottles, pipes, house-ware, toys and other objects (Kalogerakis et al., 2017; PlasticEurope, 2015). Polypropylene (PP) was also found in plastic waste MPs, confirming the relevance of this polymer as environmental contaminant and MP exposure source. Polymers such as PP, PE and PET are the main polymeric particulate materials present in the airborne environment, while most of the studies on the respiratory system were focused on the health effects of polystyrene (PS) beads (Dong et al., 2020; Xu et al., 2019; Yacobi et al., 2008). Thus, extrapolations of findings from PS materials to other polymers should be made with caution, and novel model studies should be introduced including PP, PE, and PET microplastics (Lehner et al., 2019). Furthermore, in particles originating from waste plastic, other compounds (as  $\text{TiO}_2$  and phthalocyanine, as shown in this work by Raman analysis) can be present as co-contaminants and thus, biological responses may be in part attributed to chemical toxicity resulting from the presence and release of other chemicals from the MPs in the cell culture medium during the exposure (Andrady, 2011a; Rochman, 2015). In addition, weathering and ageing processes may increase the MP reactivity, as well as the uptake of contaminants on MPs through increased surface area and polarity (Teuten et al., 2009; Wang et al., 2020). Since the wMPs of this study are obtained from end-of-life materials and have been exposed to grinding and UV radiation, they could be considered as naturally aged polymers, which might

**FIGURE 7** TEM representative images of cells exposed to wMPs (100  $\mu\text{g}/\text{ml}$ ). (A) Control cell 24 h; (B–D) cells after 24 h of exposure; (E) control cell 48 h; (F–H) cells after 48 h of exposure. N, nucleus; ERR, rough endoplasmic reticulum; G, Golgi; E, endosome; M, mitochondria; arrows indicate microplastic fragments.



have been subjected to several physico-chemical modifications able to increase their affinity for other, more dangerous compounds, among them metal ions (Andrady, 2011a). The presence of metals in wMPs samples was reported in our previous work, in which total reflection X-ray fluorescence spectrometry (TXRF) and TEM-EDX analyses showed the presence of Pb, Ti, Si and Fe, homogeneously distributed inside plastic particles (<50  $\mu\text{m}$ ) (Bonfanti et al., 2021).

The pathways suggested to be involved in MPs toxicity are oxidative stress, inflammation, disruption of immune function, translocation to circulatory system for the nanosized MPs (nanoplastics) (Hirt & Body-Malapel, 2020; Yee et al., 2021) and so the ability to induce DNA damage, posing the attention on MPs possible genotoxicity (Poma et al., 2019). Our results showed that wMPs are nontoxic at the lower concentrations, while a reduction of cell viability occurs after exposure at high concentrations (100  $\mu\text{g}/\text{ml}$ ) and for prolonged

time of exposure (48 h), as also evidenced by previous *in vitro* studies on human cells (Dong et al., 2020; Poma et al., 2019). However, in our tested conditions, no increase of intracellular ROS levels was observed in treated cells after acute exposure to wMPs. A recent publication (Gautam et al., 2022) showed that PE MPs induce ROS in several cells line, with the exception of A549 and other epithelial cells, in accordance to our findings. Furthermore, recently, other authors (Jeon et al., 2021) have reported that the weathering process, such as UV radiation, increases the intrinsic ROS associated to MPs, but also the binding of serum proteins to MPs, which can act as a ROS scavenger. Thus, since our samples are waste MPs, we can assume that they have encountered a weathering process and therefore hypothesize that serum proteins in the cell culture medium (FBS 1%) acted as ROS scavenger, resulting in lowering of intracellular ROS levels at the highest concentration of exposure.

Noticeably, even if wMPs seem to be not hazardous at low concentrations, they could exacerbate toxic effects in conjunction with other pollutants, such as airborne particulate matter (PM) and ultrafine particles (UFP) derived from diesel engines, combustion of biomass for domestic heating or from power plants. MPs, as part of PM, can indeed determine an increasing harmful effect of the PM itself, and the evaluation of risks derived from exposures to particulate is currently performed largely on an individual source of particles or chemical hazard; however, risk assessment is evolving to evaluate more closely the complexity deriving from the combined exposure to multiple chemicals (Meek et al., 2011; Moretto et al., 2016).

The effects of MPs on the inflammatory response and immune system are also of great interest, and previous works have demonstrated that PS nanoparticles lead to inflammation in rats' lungs (Brown et al., 2001) and pro-inflammatory gene expression in epithelial cells (Xu et al., 2019), as well as to the release of IL-6 and IL-8 in bronchial cells (Dong et al., 2020). Pro-inflammatory cytokines are indeed pivotal mediators involved in the activation of the immune systems (Moldoveanu et al., 2009) and considerable evidence exists that a local release of IL-6 and IL-8 in the lungs is related to the exacerbation of lung chronic diseases, such as COPD (van der Eerden, 2019) and asthma (MacNee, 2001). Our data show that IL-6 and IL-8 release from A549 cells is increased after the exposure to high concentration of wMPs (100 µg/ml) at 48 h.

It has to be taken into account that the release of inflammatory mediators could be due to the persistence of microorganisms or bacterial components, such as lipopolysaccharides (LPS), on MPs surface, acting as a vector for these organisms (Oberbeckmann et al., 2015). Moreover, diverse communities of bacteria have been identified in airborne PM (Franzetti et al., 2010; Gualtieri et al., 2011), and the role of endotoxins in leading the PM inflammatory responses has been well reported (Camatini et al., 2012; Kocbach et al., 2008). Thus, the content of endotoxins in the wMPs samples was tested by Limulus amoebocyte lysate (LAL) test and was of  $0.044 \pm 0.003$  EU/mg, which can be considered very low compared to other PM samples, such as summer PM<sub>10</sub>, in which the amount of endotoxin able to induce a significant inflammatory response in lung cells was quite high (25 EU/mg) (Longhin et al., 2013). This result suggests the involvement of other components in the induction of inflammatory mediator release by wMPs exposure, rather than the endotoxins contribution, and overall our data further enlighten the importance to investigate the potential inflammatory effect of inhaled MPs, since inflammation has been indeed identified as a key molecular event (KE149) involved in the putative adverse outcome pathways (AOPs) for MPs (Jeong & Choi, 2020). Beside inflammatory responses, our data about cellular and nuclear morphology pointed out that high concentration of wMPs are able to induce some cellular morphological changes even at shorter time of exposure, such as the formation of micronuclei and nuclear buds, as well as evidence of mitotic catastrophe, which are visible in cells treated for 24 h with MPs. The capability of wMPs to induce DNA damage and genotoxic response was further investigated at 48 h of exposure to high concentration of particles by performing the *in vitro* mammalian cell micronucleus (MN) test following the

OECD guideline for the testing of chemicals (OECD, 2016). Data showed increased levels of MNs and NBUDs in A549 cells, demonstrating that the interaction between cells and MPs leads to cellular DNA damage, in accordance with the work of Poma and colleagues, in which PS nanoparticles (PNPs) induced genotoxicity with an increased number of micronuclei in fibroblast cells (Poma et al., 2019).

Immunofluorescence microscopy images of cells exposed to wMPs showed that cellular uptake occurs for the smallest subfractions (<5 µm); wMPs stained with Nile Red are mapped inside the cytoplasm, near the nucleus. Although not properly defined as phagocytic cells, A549 cells are indeed able to activate endocytosis and even phagocytosis processes, when exposed to particulate materials (Dominici et al., 2013; Gualtieri et al., 2009; Singh et al., 2007). We thus consider this cell line either for the representativeness as biological target and the capability of MPs uptake. However, just to compare the effects with an additional cell line, preliminary experiments were performed to investigate the impact of wMPs in Balb/3 T3 fibroblasts. Both cell viability, assessed by MTT, and cell morphology through fluorescence microscopy were analysed (Figures S11 and S12). Data show that there is reduction of Balb/3T3 cell viability after high concentrations (100 µg/ml) for prolonged time (48 h), though not significant. Immunofluorescence images indeed showed that MPs did not induce fibroblast morphological changes, neither fluorescent wMPs are clearly detectable. This result suggests that fibroblast cells are less sensitive to environmental wMPs compared to lung epithelial cells.

Further demonstration of wMPs cellular uptake by A549 cells was evidenced by TEM and confocal µRaman spectroscopy imaging: This last technique allows the identification of different sub-cellular regions, as well as the cell-nanoparticle interactions (Byrne et al., 2020; Chernenko et al., 2009; Dorney et al., 2012; Efeoglu et al., 2016), and the analysis showed that particles with strong fluorescent signal were found in cells, inside the cytoplasm and, in some cases, near to the nucleus, enlightening that the smallest fraction of wMPs (<5 µm) can be internalized by lung cells, as previously shown in A549 cells (Xu et al., 2019) and in rat alveolar epithelial cells (Yacobi et al., 2008) through confocal microscopy. The interaction with the tested wMPs induced cytoskeleton remodelling, as evidenced by disassembled actin fibres, and these morphological changes have been evidenced also in A549 cells exposed to insoluble metal oxide nanoparticles, such as TiO<sub>2</sub> (Bengalli et al., 2019). Moreover, the contact of MPs with the plasma membrane could cause a mechanical stretching on the lipid bilayer, leading to potential severe cell machinery dysfunction (Fleury & Baulin, 2021): Hydrophobic nanoparticles are indeed incorporated in the membrane lipid bilayer (Foroozandeh & Aziz, 2018), and this interaction may cause an increase of Ca<sup>2+</sup> influx inducing a signalling cascade that impacts on cytoskeleton organization (Hussain et al., 2014).

Nevertheless, further investigations are needed to clarify the real contribution of the polymeric component itself or of other contaminants, on wMPs cytotoxicity, similarly on the mechanism of action in target cells. In particular, the role of oxidative stress in the wMPs induced effects, as well as biomarkers that evoke specific mode of

actions (MoA) and consequent AOPs related to MPs exposure, need to be still elucidated.

Moreover, since several criticisms could arise during the testing of MPs, due to the peculiar physico-chemical properties of the different polymers, in the future, it will be crucial to validate and standardize new methods and technologies for the collection, detection, characterization, samples preparation, dispersion and toxicological testing protocols for a correct evaluation of the toxicity of these emerging environmental contaminants.

Therefore, the overall results indicate that lung cells are affected by exposure to wMPs when administered at high dosages. Nevertheless, since few particles are visible on the cells and their size is about 1–2  $\mu\text{m}$ , it is conceivable that the observed results could be due to persistent pollutants present on the MPs surface or to the release of additives, dyes or other compounds from particles (Campanale et al., 2020), including soluble metals or insoluble particles fraction (surface defects), that could be responsible of ROS formation and consequent oxidative DNA damage (Schins & Knaapen, 2008).

## 5 | CONCLUSIONS

Considering the mounting evidences on the relevant MPs presence in the aerosol, especially in indoor air, more stringent efforts to characterize human exposure and inhalation toxicity of MPs are necessary, also in the view of distilling their possible role in inducing lesions to cells lining the respiratory system and in air pollution-associated respiratory diseases.

In this context, the bio-interactions among cells and MPs, with consequent mechanical stress at cell surface level, followed by intracellular signal transduction culminating in inflammatory responses and DNA damage, coupled with the ability of sub-micrometric particles to be uptaken by cells, represent crucial steps to be investigated in the MP-induced AOPs. Currently, airborne micrometric MPs, founded and monitored in PM samples, have similar size to the ones tested in this work.

In vitro toxicology is useful in clarifying the mechanisms and modes of action of MPs in inducing pathologies; our study provides a substantive contribution in this direction, focusing for the first time on the effects induced in human lung cells by waste-derived MPs. These MPs are composed by a polymer mixture (mainly PE and PP), characterized by polymorphic and different in size, including fibre-shaped ones, together with associated chemicals and other co-contaminants. Our results show that, similarly to other commercial or lab-produced MPs, wMPs displayed a moderate acute toxicity in vitro, with appreciable biological effects only after exposure to high concentrations and prolonged exposure time. Sub-toxic effects consisting in cytoskeletal rearrangement and genotoxicity, likely due to the surface interactions and particle uptake by cells, were also observed, ringing the bell for possible chronic adverse outcomes in consequence of the persistency of such insoluble MPs.

wMPs are quite big in size, compared to PM inhaled particles. Since in the next years the methods of detection and quantification of

fine (sub-micrometric) MPs will definitely improve, it will be crucial to focus and improve the research about toxicological effects of reference standard environmental MPs.

These results point out the importance to monitor the real amount of airborne MPs in the atmosphere, in indoor and outdoor environments and to perform hazard assessment in parallel, in order to better define the risk for MPs exposure.

## ACKNOWLEDGEMENTS

The research leading to these results resulted from the access to the Nanobiotechnology Laboratory under the framework of the Research Infrastructure Access Agreement No. 35559/14, 2019-1- RD -Nanobiotech, of the European Commission. The authors thank Drs. Alessia Bogni, Pascal Colpo, Giacomo Ceccone and Francesco Fumagalli, European Commission, Joint Research Centre – Ispra, for the fruitful discussion. The authors wish to thank the colleagues from University of Milano-Bicocca, Dr. G. Baeri, A. Colantuoni, G. Motta and A. Colombo and L. Fiandra for their precious help in MPs preparation and editing and Dr. T. Catelani, microscopy facility, for assistance in SEM analyses. Open Access Funding provided by Università degli Studi di Milano-Bicocca within the CRUI-CARE Agreement.

## CONFLICTS OF INTEREST

The authors have no conflict of interest to report.

## DISCLAIMER

The information and views set out in this publication are those of the author(s) and do not necessarily reflect the official opinion of the European Union. Neither the European Union institutions and bodies nor any person acting on their behalf may be held responsible for the use that may be made of the information contained therein.

## ORCID

Rossella Bengalli  <https://orcid.org/0000-0002-9657-2016>

Paride Mantecca  <https://orcid.org/0000-0002-6962-049X>

## REFERENCES

- Allen, S., Allen, D., Phoenix, V. R., le Roux, G., Durántez Jiménez, P., Simonneau, A., Binet, S., & Galop, D. (2019). Atmospheric transport and deposition of microplastics in a remote mountain catchment. *Nature Geoscience*, 12(5), 339–344. <https://doi.org/10.1038/s41561-019-0335-5>
- Amato, F., Karanasiou, A., Moreno, T., Alastuey, A., Orza, J. A. G., Lumbreras, J., Borge, R., Boldo, E., Linares, C., & Querol, X. (2012). Emission factors from road dust resuspension in a Mediterranean free-way. *Atmospheric Environment*, 61, 580–587. <https://doi.org/10.1016/j.atmosenv.2012.07.065>
- Andrady, A. L. (2011a). Microplastics in the marine environment. *Marine Pollution Bulletin*, 62(8), 1596–1605. <https://doi.org/10.1016/j.marpolbul.2011.05.030>
- Andrady, A. L. (2011b). Using flow cytometry to detect micro- and nano-scale polymer particles. Proceedings of the Second Research Workshop on Microplastic Marine Debris. NOAA Technical Memorandum NOS-OR&R-39.
- Asamany, E. A., Gibson, M. D., & Pegg, M. J. (2017). Evaluating the potential of waste plastics as fuel in cement kilns using bench-scale

- emissions analysis. *Fuel*, 193, 178–186. <https://doi.org/10.1016/J.FUEL.2016.12.054>
- Barboza, L. G. A., Dick Vethaak, A., Lavorante, B. R. B. O., Lundebye, A. K., & Guilhermino, L. (2018). Marine microplastic debris: An emerging issue for food security, food safety and human health. *Marine Pollution Bulletin*, 133, 336–348. <https://doi.org/10.1016/J.MARPOLBUL.2018.05.047>
- Bengalli, R., Ortelli, S., Blosi, M., Costa, A., Mantecca, P., & Fiandra, L. (2019). In vitro toxicity of TiO<sub>2</sub>:SiO<sub>2</sub> nanocomposites with different photocatalytic properties. *Nanomaterials*, 9(7). <https://doi.org/10.3390/NANO9071041>
- Bonfanti, P., Colombo, A., Saibene, M., Motta, G., Saliu, F., Catelani, T., ... Mantecca, P. (2021). Microplastics from miscellaneous plastic wastes: Physico-chemical characterization and impact on fish and amphibian development. *Ecotoxicology and Environmental Safety*, 225, 112775. <https://doi.org/10.1016/J.ECOENV.2021.112775>
- Brown, D. M., Wilson, M. R., MacNee, W., Stone, V., & Donaldson, K. (2001). Size-dependent proinflammatory effects of ultrafine polystyrene particles: A role for surface area and oxidative stress in the enhanced activity of Ultrafines. *Toxicology and Applied Pharmacology*, 175(3), 191–199. <https://doi.org/10.1006/TAAP.2001.9240>
- Byrne, H. J., Bonnier, F., Efeoglu, E., Moore, C., & McIntyre, J. (2020). In vitro label free Raman microspectroscopic analysis to monitor the uptake, fate and impacts of nanoparticle based materials. *Frontiers in Bioengineering and Biotechnology*, 8, 1277. <https://doi.org/10.3389/FBIOE.2020.544311>
- Cai, L., Wang, J., Peng, J., Tan, Z., Zhan, Z., Tan, X., & Chen, Q. (2017). Characteristic of microplastics in the atmospheric fallout from Dongguan city, China: Preliminary research and first evidence. *Environmental Science and Pollution Research*, 24(32), 24928–24935. <https://doi.org/10.1007/s11356-017-0116-x>
- Camatini, M., Corvaja, V., Pezzolato, E., Mantecca, P., & Gualtieri, M. (2012). PM10-biogenic fraction drives the seasonal variation of proinflammatory response in A549 cells. *Environmental Toxicology*, 27(2), 63–73. <https://doi.org/10.1002/TOX.20611>
- Campanale, C., Massarelli, C., Savino, I., Locaputo, V., & Uricchio, V. F. (2020). A detailed review study on potential effects of microplastics and additives of concern on human health. *International Journal of Environmental Research and Public Health*, 17(4), 1212. <https://doi.org/10.3390/IJERPH17041212>
- Capuano, L., Magatti, G., Perucca, M., Dettori, M., & Mantecca, P. (2020). Use of recycled plastics as a second raw material in the production of road pavements: An example of circular economy evaluated with LCA methodology. *Procedia Environmental Science, Engineering and Management*, 7, 37–43. PMID: Retrieved from <http://www.procedia-esem.eu>
- Chernenko, T., Matthäus, C., Milane, L., Quintero, L., Amiji, M., & Diem, M. (2009). Label-free Raman spectral imaging of intracellular delivery and degradation of polymeric nanoparticle systems. *ACS Nano*, 3(11), 3552–3559. <https://doi.org/10.1021/NN9010973>
- Collignon, A., Hecq, J. H., Galgani, F., Collard, F., & Goffart, A. (2014). Annual variation in neustonic micro- and meso-plastic particles and zooplankton in the bay of Calvi (Mediterranean–Corsica). *Marine Pollution Bulletin*, 79(1–2), 293–298. <https://doi.org/10.1016/J.MARPOLBUL.2013.11.023>
- Cowger, W., Steinmetz, Z., Gray, A., Munno, K., Lynch, J., Hapich, H., Primpke, S., de Frond, H., Rochman, C., & Herodotou, O. (2021). Microplastic spectral classification needs an open source community: Open Specy to the rescue! *Analytical Chemistry*, 93(21), 7543–7548. <https://doi.org/10.1021/ACS.ANALCHEM.1C00123>
- Dominici, L., Guerrero, E., Villarini, M., Fatigoni, C., Moretti, M., Blasi, P., & Monarca, S. (2013). Evaluation of in vitro cytotoxicity and genotoxicity of size-fractionated air particles sampled during road tunnel construction. *BioMed Research International*, 2013, 1–9. <https://doi.org/10.1155/2013/345724>
- Dong, C. D., Chen, C. W., Chen, Y. C., Chen, H. H., Lee, J. S., & Lin, C. H. (2020). Polystyrene microplastic particles: In vitro pulmonary toxicity assessment. *Journal of Hazardous Materials*, 385, 121575. <https://doi.org/10.1016/j.jhazmat.2019.121575>
- Dorney, J., Bonnier, F., Garcia, A., Casey, A., Chambers, G., & Byrne, H. J. (2012). Identifying and localizing intracellular nanoparticles using Raman spectroscopy. *Analyst*, 137(5), 1111–1119. <https://doi.org/10.1039/C2AN15977E>
- Dris, R., Gasperi, J., Mirande, C., Mandin, C., Guerrouache, M., Langlois, V., & Tassin, B. (2017). A first overview of textile fibers, including microplastics, in indoor and outdoor environments. *Environmental Pollution*, 221, 453–458. <https://doi.org/10.1016/J.ENVPOL.2016.12.013>
- Dris, R., Gasperi, J., Rocher, V., Saad, M., Renault, N., & Tassin, B. (2015). Microplastic contamination in an urban area: A case study in Greater Paris. *Environmental Chemistry*, 12(5), 592–599. <https://doi.org/10.1071/EN14167>
- Dris, R., Gasperi, J., Saad, M., Mirande, C., & Tassin, B. (2016). Synthetic fibers in atmospheric fallout: A source of microplastics in the environment? *Marine Pollution Bulletin*, 104(1–2), 290–293. <https://doi.org/10.1016/j.marpolbul.2016.01.006>
- EAPA. (2017). Position statement on the use of secondary materials, by-products and waste in asphalt mixtures. Retrieved August 5, 2021, from <https://eapa.org/wp-content/uploads/2019/12/TF-RA-19-N006-EAPA-Position-Statement-on-the-Use-of-Secondary-Materials-By-products-and-Waste-in-Asphalt-Mixtures-2017.pdf>
- Efeoglu, E., Casey, A., & Byrne, H. J. (2016). In vitro monitoring of time and dose dependent cytotoxicity of aminated nanoparticles using Raman spectroscopy. *Analyst*, 141(18), 5417–5431. <https://doi.org/10.1039/C6AN01199C>
- EFSA Panel on Contaminants in the Food Chain (CONTAM). (2016). Presence of microplastics and nanoplastics in food, with particular focus on seafood. *EFSA Journal*, 14(6). <https://doi.org/10.2903/J.EFSA.2016.4501>
- Erni-Cassola, G., Gibson, M. I., Thompson, R. C., & Christie-Oleza, J. A. (2017). Lost, but found with Nile red: A novel method for detecting and quantifying small microplastics (1 mm to 20 μm) in environmental samples. *Environmental Science and Technology*, 51(23), 13641–13648. <https://doi.org/10.1021/ACS.EST.7B04512>
- European Commission. (2018). An European strategy for plastics in a circular economy.
- Fendall, L. S., & Sewell, M. A. (2009). Contributing to marine pollution by washing your face: Microplastics in facial cleansers. *Marine Pollution Bulletin*, 58(8), 1225–1228. <https://doi.org/10.1016/j.marpolbul.2009.04.025>
- Fenech, M. (2007). Cytokinesis-block micronucleus cytome assay. *Nature Protocols*, 2(5), 1084–1104. <https://doi.org/10.1038/nprot.2007.77>
- Fleury, J.-B., & Baulin, V. A. (2021). Microplastics destabilize lipid membranes by mechanical stretching. *Proceedings of the National Academy of Sciences*, 118(31). <https://doi.org/10.1073/PNAS.2104610118>
- Foroozandeh, P., & Aziz, A. A. (2018). Insight into cellular uptake and intracellular trafficking of nanoparticles. *Nanoscale Research Letters*, 13(1), 1–12. <https://doi.org/10.1186/S11671-018-2728-6>
- Franzetti, A., Gandolfi, I., Gaspari, E., Ambrosini, R., & Bestetti, G. (2010). Seasonal variability of bacteria in fine and coarse urban air particulate matter. *Applied Microbiology and Biotechnology*, 90(2), 745–753. <https://doi.org/10.1007/S00253-010-3048-7>
- Gasperi, J., Wright, S. L., Dris, R., Collard, F., Mandin, C., Guerrouache, M., Langlois, V., Kelly, F. J., & Tassin, B. (2018). Microplastics in air: Are we breathing it in? *Current Opinion in Environmental Science & Health*, 1, 1–5. <https://doi.org/10.1016/j.coesh.2017.10.002>
- Gautam, R., Jo, J. H., Acharya, M., Maharjan, A., Lee, D. E., K.C., P. B., Kim, C. Y., Kim, K. S., Kim, H. A., & Heo, Y. (2022). Evaluation of potential toxicity of polyethylene microplastics on human derived cell lines.

- Science of the Total Environment*, 838, 156089. <https://doi.org/10.1016/J.SCITOTENV.2022.156089>
- Gigault, J., ter Halle, A., Baudrimont, M., Pascal, P.-Y., Gauffre, F., Phi, T.-L., el Hadri, H., Grassl, B., & Reynaud, S. (2018). Current opinion: What is a nanoplastic? *Environmental Pollution (Barking, Essex: 1987)*, 235, 1030–1034. <https://doi.org/10.1016/j.envpol.2018.01.024>
- Grady, B. P. (2021). Waste plastics in asphalt concrete: A review. *SPE Polymers*, 2(1), 4–18. <https://doi.org/10.1002/PLS2.10034>
- Gualtieri, M., Franzetti, A., Longhin, E., Mantecca, P., Bestetti, G., Bolzacchini, E., & Camatini, M. (2011). In vitro effects of microbiologically characterized Milan particulate matter. *Procedia Environmental Sciences*, 4, 192–197. <https://doi.org/10.1016/J.PROENV.2011.03.023>
- Gualtieri, M., Mantecca, P., Corvaja, V., Longhin, E., Perrone, M. G., Bolzacchini, E., & Camatini, M. (2009). Winter fine particulate matter from Milan induces morphological and functional alterations in human pulmonary epithelial cells (A549). *Toxicology Letters*, 188(1), 52–62. <https://doi.org/10.1016/J.TOXLET.2009.03.003>
- Hirt, N., & Body-Malapel, M. (2020). Immunotoxicity and intestinal effects of nano- and microplastics: A review of the literature. *Particle and Fibre Toxicology*, 17(1), 1–22. <https://doi.org/10.1186/S12989-020-00387-7>
- Hussain, S., Garantziotis, S., Rodrigues-Lima, F., Dupret, J., Baeza-Squiban, A., & Boland, B. (2014). Intracellular signal modulation by nanomaterials. *Advances in Experimental Medicine and Biology*, 811, 113–134. [https://doi.org/10.1007/978-94-017-8739-0\\_7](https://doi.org/10.1007/978-94-017-8739-0_7)
- Jeon, S., Lee, D. K., Jeong, J., Yang, S. I., Kim, J. S., Kim, J., & Cho, W. S. (2021). The reactive oxygen species as pathogenic factors of fragmented microplastics to macrophages. *Environmental Pollution*, 281, 117006. <https://doi.org/10.1016/J.ENVPOL.2021.117006>
- Jeong, J., & Choi, J. (2020). Development of AOP relevant to microplastics based on toxicity mechanisms of chemical additives using ToxCast™ and deep learning models combined approach. *Environment International*, 137, 105557. <https://doi.org/10.1016/j.envint.2020.105557>
- Kalogerakis, N., Karkanorachaki, K., Kalogerakis, G. C., Triantafyllidi, E. I., Gotsis, A. D., Partsinevelos, P., & Fava, F. (2017). Microplastics generation: Onset of fragmentation of polyethylene films in marine environment mesocosms. *Frontiers in Marine Science*, 4(MAR), 84. <https://doi.org/10.3389/FMARS.2017.00084>
- Kocbach, A., Totlandsdal, A. I., Låg, M., Refsnes, M., & Schwarze, P. E. (2008). Differential binding of cytokines to environmentally relevant particles: A possible source for misinterpretation of in vitro results? *Toxicology Letters*, 176(2), 131–137. <https://doi.org/10.1016/J.TOXLET.2007.10.014>
- Lehner, R., Weder, C., Petri-Fink, A., & Rothen-Rutishauser, B. (2019). Emergence of nanoplastic in the environment and possible impact on human health. *Environmental Science & Technology*, 53(4), 1748–1765. <https://doi.org/10.1021/ACS.EST.8B05512>
- Longhin, E., Pezzoloto, E., Mantecca, P., Holme, J. A., Franzetti, A., Camatini, M., & Gualtieri, M. (2013). Season linked responses to fine and quasi-ultrafine Milan PM in cultured cells. *Toxicology in Vitro*, 27(2), 551–559. <https://doi.org/10.1016/J.TIV.2012.10.018>
- MacNee, W. (2001). Oxidative stress and lung inflammation in airways disease. *European Journal of Pharmacology*, 429(1–3), 195–207. [https://doi.org/10.1016/S0014-2999\(01\)01320-6](https://doi.org/10.1016/S0014-2999(01)01320-6)
- Maes, T., Jessop, R., Wellner, N., Haupt, K., & Mayes, A. G. (2017). A rapid-screening approach to detect and quantify microplastics based on fluorescent tagging with Nile Red. *Scientific Reports*, 7(1), 1–10. <https://doi.org/10.1038/srep44501>
- Matthias, T., & Hengstmann, E. E. K. F. (2017). Nile red staining as a subsidiary method for microplastic quantification: A comparison of three solvents and factors influencing application reliability. *SDRP Journal of Earth Sciences & Environmental Studies*, 2(2). <https://doi.org/10.25177/JESES.2.2.1>
- Meek, M., Boobis, A., Crofton, K., Heinemeyer, G., Raaij, M., & Vickers, C. (2011). Risk assessment of combined exposure to multiple chemicals: A WHO/IPCS framework. *Regulatory Toxicology and Pharmacology: RTP*, 60(2), S1–S14. <https://doi.org/10.1016/J.YRTPH.2011.03.010>
- Moldoveanu, B., Otmishi, P., Jani, P., Walker, J., Sarmiento, X., Guardiola, J., Saad, M., & Yu, J. (2009). Inflammatory mechanisms in the lung. *Journal of Inflammation Research*, 2, 1. PMID: Retrieved from [pmc/articles/PMC3218724/](https://pubmed.ncbi.nlm.nih.gov/193218724/).
- Moore, C. J. (2008). Synthetic polymers in the marine environment: A rapidly increasing, long-term threat. *Environmental Research*, 108(2), 131–139. <https://doi.org/10.1016/j.envres.2008.07.025>
- Moretto, A., Bachman, A., Boobis, A., Solomon, K. R., Pastoor, T. P., Wilks, M. F., & Embry, M. R. (2016). A framework for cumulative risk assessment in the 21st century. *Critical Reviews in Toxicology*, 47(2), 85–97. <https://doi.org/10.1080/10408444.2016.1211618>
- Mosmann, T. (1983). Rapid colorimetric assay for cellular growth and survival: Application to proliferation and cytotoxicity assays. *Journal of Immunological Methods*, 65(1–2), 55–63. [https://doi.org/10.1016/0022-1759\(83\)90303-4](https://doi.org/10.1016/0022-1759(83)90303-4)
- Oberbeckmann, S., Löder, M. G. J., Labrenz, M., Oberbeckmann, S., Löder, M. G. J., & Labrenz, M. (2015). Marine microplastic-associated biofilms—A review. *Environmental Chemistry*, 12(5), 551–562. <https://doi.org/10.1071/EN15069>
- OECD. (2016). Test No. 487: In vitro mammalian cell micronucleus test.
- PlasticEurope. (2015). An analysis of European plastics production, demand and waste data.
- Poma, A., Vecchiotti, G., Colafarina, S., Zarivi, O., Aloisi, M., Arrizza, L., Chichiriccò, G., & di Carlo, P. (2019). In vitro genotoxicity of polystyrene nanoparticles on the human fibroblast HS27 cell line. *Nanomaterials*, 9(9). <https://doi.org/10.3390/nano9091299>
- Prata, J. C. (2018). Airborne microplastics: Consequences to human health? *Environmental Pollution*, 234, 115–126. <https://doi.org/10.1016/j.envpol.2017.11.043>
- Prata, J. C., da Costa, J. P., Lopes, I., Duarte, A. C., & Rocha-Santos, T. (2020). Environmental exposure to microplastics: An overview on possible human health effects. *The Science of the Total Environment*, 702, 134455. <https://doi.org/10.1016/j.scitotenv.2019.134455>
- Rochman, C. M. (2015). The complex mixture, fate and toxicity of chemicals associated with plastic debris in the marine environment. *Marine Anthropogenic Litter*, 117–140. [https://doi.org/10.1007/978-3-319-16510-3\\_5](https://doi.org/10.1007/978-3-319-16510-3_5)
- Schins, R. P. F., & Knaapen, A. M. (2008). Genotoxicity of poorly soluble particles. *Inhalation Toxicology*, 19(SUPPL. 1), 189–198. <https://doi.org/10.1080/08958370701496202>
- Schymanski, D., Goldbeck, C., Humpf, H. U., & Fürst, P. (2018). Analysis of microplastics in water by micro-Raman spectroscopy: Release of plastic particles from different packaging into mineral water. *Water Research*, 129, 154–162. <https://doi.org/10.1016/J.WATRES.2017.11.011>
- Shim, W. J., Song, Y. K., Hong, S. H., & Jang, M. (2016). Identification and quantification of microplastics using Nile red staining. *Marine Pollution Bulletin*, 113(1–2), 469–476. <https://doi.org/10.1016/J.MARPOLBUL.2016.10.049>
- Shim, W. J., & Thomposon, R. C. (2015). Microplastics in the ocean. *Archives of Environmental Contamination and Toxicology*, 69(3), 265–268. <https://doi.org/10.1007/s00244-015-0216-x>
- Simon, S., & Röhrs, S. (2018). Between fakes, forgeries, and illicit artifacts—Authenticity studies in a heritage science laboratory. *Art*, 7(2), 20. <https://doi.org/10.3390/arts7020020>
- Singh, S., Shi, T., Duffin, R., Albrecht, C., van Berlo, D., Höhr, D., Fubini, B., Martra, G., Fenoglio, I., Borm, P. J., & Schins, R. P. F. (2007). Endocytosis, oxidative stress and IL-8 expression in human lung epithelial cells upon treatment with fine and ultrafine TiO<sub>2</sub>: Role of the specific surface area and of surface methylation of the particles. *Toxicology and*

- Applied Pharmacology*, 222(2), 141–151. <https://doi.org/10.1016/J.TAAP.2007.05.001>
- Sommer, F., Dietze, V., Baum, A., Sauer, J., Gilge, S., Maschowski, C., & Gieré, R. (2018). Tire abrasion as a major source of microplastics in the environment. *Aerosol and Air Quality Research*, 18(8), 2014–2028. <https://doi.org/10.4209/AAQR.2018.03.0099>
- Stanton, T., Johnson, M., Nathanail, P., Gomes, R. L., Needham, T., & Burson, A. (2019). Exploring the efficacy of Nile Red in microplastic quantification: A costaining approach. *Environmental Science & Technology Letters*, 6(10), 606–611. <https://doi.org/10.1021/ACS.ESTLETT.9B00499>
- Teuten, E. L., Rowland, S. J., Galloway, T. S., & Thompson, R. C. (2007). Potential for plastics to transport hydrophobic contaminants. *Environmental Science & Technology*, 41(22), 7759–7764. <https://doi.org/10.1021/es071737s>
- Teuten, E. L., Saquing, J. M., Knappe, D. R. U., Barlaz, M. A., Jonsson, S., Björn, A., Rowland, S. J., Thompson, R. C., Galloway, T. S., Yamashita, R., Ochi, D., Watanuki, Y., Moore, C., Viet, P. H., Tana, T. S., Prudente, M., Boonyatumanond, R., Zakaria, M. P., Akkhang, K., ... Takada, H. (2009). Transport and release of chemicals from plastics to the environment and to wildlife. *Philosophical Transactions of the Royal Society, B: Biological Sciences*, 364(1526), 2027–2045. <https://doi.org/10.1098/RSTB.2008.0284>
- Thomas, P., Umegaki, K., & Fenech, M. (2003). Nucleoplasmic bridges are a sensitive measure of chromosome rearrangement in the cytokinesis-block micronucleus assay. *Mutagenesis*, 18(2), 187–194. <https://doi.org/10.1093/mutage/18.2.187>
- van der Eerden, M. M. (2019). Mediators of inflammation in COPD. *Pulmonary Medicine and Respiratory Research*, 5(2), 1–10. <https://doi.org/10.24966/PMRR-0177/100026>
- Walton, W. H. (1948). Feret's statistical diameter as a measure of particle size. *Nature*, 162(4113), 329–330. <https://doi.org/10.1038/162329b0>
- Wang, F., Wong, C. S., Chen, D., Lu, X., Wang, F., & Zeng, E. Y. (2018). Interaction of toxic chemicals with microplastics: A critical review. *Water Research*, 139, 208–219. <https://doi.org/10.1016/J.WATRES.2018.04.003>
- Wang, Q., Zhang, Y., Wangjin, X., Wang, Y., Meng, G., & Chen, Y. (2020). The adsorption behavior of metals in aqueous solution by microplastics effected by UV radiation. *Journal of Environmental Sciences*, 87, 272–280. <https://doi.org/10.1016/J.JES.2019.07.006>
- Worm, B., Lotze, H. K., Jubinville, I., Wilcox, C., & Jambeck, J. (2017). Plastic as a persistent marine pollutant. *Annual Review of Environment and Resources*, 42(1), 1–26. <https://doi.org/10.1146/annurev-environ-102016-060700>
- Wright, S. L., & Kelly, F. J. (2017). Plastic and human health: A micro issue? *Environmental Science and Technology*, 51(12), 6634–6647. <https://doi.org/10.1021/acs.est.7b00423>
- Xu, M., Halimu, G., Zhang, Q., Song, Y., Fu, X., Li, Y., Li, Y., & Zhang, H. (2019). Internalization and toxicity: A preliminary study of effects of nanoplastic particles on human lung epithelial cell. *Science of the Total Environment*, 694, 133794. <https://doi.org/10.1016/J.SCITOTENV.2019.133794>
- Yacobi, N. R., DeMaio, L., Xie, J., Hamm-Alvarez, S. F., Borok, Z., Kim, K. J., & Crandall, E. D. (2008). Polystyrene nanoparticle trafficking across alveolar epithelium. *Nanomedicine: Nanotechnology, Biology, and Medicine*, 4(2), 139–145. <https://doi.org/10.1016/j.nano.2008.02.002>
- Yee, M. S.-L., Hii, L.-W., Looi, C. K., Lim, W.-M., Wong, S.-F., Kok, Y.-Y., Tan, B. K., Wong, C. Y., & Leong, C.-O. (2021). Impact of microplastics and nanoplastics on human health. *Nanomaterials*, 11(2), 496. <https://doi.org/10.3390/NANO11020496>

## SUPPORTING INFORMATION

Additional supporting information can be found online in the Supporting Information section at the end of this article.

**How to cite this article:** Bengalli, R., Zerboni, A., Bonfanti, P., Saibene, M., Mehn, D., Cella, C., Ponti, J., La Spina, R., & Mantecca, P. (2022). Characterization of microparticles derived from waste plastics and their bio-interaction with human lung A549 cells. *Journal of Applied Toxicology*, 42(12), 2030–2044. <https://doi.org/10.1002/jat.4372>